 

PACS numbers: 34.80.Dp; 39.20.+j
DOI: 10.1070/QE2000v030n11ABEH001855

# Excitation of Fe I and Fe II in electron – atom collisions

Yu M Smirnov

**Abstract. Excitation of the presumed laser levels of Fe I and Fe II in electron – atom collisions is studied by the techniques of extended intersecting beams and optical spectroscopy. The total excitation cross sections for the $z\,^5P_3^o$, $x\,^5D_4^o$, and $z\,^5F_5^o$ levels of the iron atom were determined. The excitation cross sections were measured for transitions arising from the odd levels of Fe II with an excitation energy ranging from 38 000 to 48 000 cm$^{-1}$ relative to the ground level of Fe II.**

## 1. Introduction

The feasibility of lasing on the transitions of atomic iron was first considered in Refs [1, 2]. The probability of lasing on the resonance-to-metastable $a\,^5P_3 - z\,^5P_3^o$ (868.863 nm) and $a\,^5F_5 - z\,^5F_5^o$ (501.207 nm) transitions was shown to be highest. However, lasing in the experimental studies that followed [3, 4] was obtained on the $a\,^5P_3 - x\,^5D_4^o$ transition (452.862 nm) instead of the expected ones. This situation was analysed in Ref. [4] on the basis of the available data on the atomic constants of Fe I. Starting from the criterion $B_{ki} \sim \lambda^3 A_{ki} q_{\max}$, which characterises the gain on the $k \to i$ transition, the authors of paper [4] showed that lasing was most likely to occur on precisely the 452.862-nm line. [Here, $\lambda$ is the wavelength of the laser transition, $A_{ki}$ is the $k \to i$ transition probability, and $q_{\max}$ is the excitation cross section for the $k$ level at the maximum of the optical excitation function (OEF)].

At the same time, the authors of [4] pointed out two primary difficulties that had to be overcome to obtain intense lasing on the transition in question. These difficulties arise from the fact that the $x\,^5D_4^o$ level is located 39625.80 cm$^{-1}$ above the $a\,^5D_4$ ground level, and therefore its efficient excitation in a discharge requires a higher electron temperature as compared with other metal vapour lasers. Moreover, the $x\,^5D_4^o$ level lifetime for the working channel is only 50 ns, with the consequence that stringent requirements are imposed on the excitation system as regards the steepness of the edge of a current pulse.

Note also that the data on atomic constants employed in the analysis performed in Ref. [4] are not reliable. The transition probabilities were borrowed from Ref. [5], in which the magnitudes of $A_{ki}$ are, as a rule, substantially different from the results of other investigations. In addition, the excitation cross sections used in Ref. [4] were obtained from an approximate formula.

There exists the possibility of obtaining lasing not only on the transitions of Fe I discussed above, but also on the transitions of a singly charged iron ion. In [6], the possibility of using the reaction of asymmetric charge exchange

$$A^+ + B \to A + B^{+*} + \Delta E, \qquad (1)$$

to obtain lasing was considered. Here, A and B are the atoms of a rare gas and a transition metal, respectively. The prospects of obtaining population inversion on the transitions of ions Sc II, Ti II, V II, Cr II, Mn II, Fe II, Co II, Ni II, Cu II, and Zn II ion in a hollow cathode discharge were discussed. In particular, radiation amplification was realised [7] for several transitions arising from a group of high-lying levels of singly charged iron ions (102000 – 10000 cm$^{-1}$ above the ground level of Fe II) in a Fe – Ne mixture discharge.

One can expect that new significant results in studies of iron vapour lasers can be achieved by employing electron-beam pumping. Recently [8], a physicomathematical model of a laser utilising manganese vapour mixed with helium (neon) was presented, in which the pumping was accomplished with a beam of electrons with an energy of several kiloelectronvolts. The efficiency and the energy output of this laser were shown to exceed those of gas-discharge systems by one-two orders of magnitude. At the same time, the authors state, 'Since the mechanisms of excitation of electron-beam-pumped lasers differ considerably from those of gas-discharge lasers, the metal atom that is most efficient for lasing in an electron-beam-pumped laser is not necessarily the best for a gas-discharge laser' (Ref. [8], p. 953).

Therefore, it is interesting to consider an iron vapour laser excited by an electron beam. However, not only the construction of a physicomathematical model, but even reliable simple estimates are hindered by the lack of information on the atomic constants of Fe I and Fe II. In recent years, especially in relation to the solution of astrophysical problems, there appeared a more reliable and extensive information on the energy level lifetimes and transition probabilities of Fe I and Fe II. However, until the present time the data on the electron-beam excitation cross sections for these objects have been lacking almost completely. The aim of this paper is to alleviate this deficiency.

**Yu M Smirnov** Moscow State Power Institute (Technical University), Krasnokazarmennaya ul. 14, 111250 Moscow, Russia

Received 24 April 2000
*Kvantovaya Elektronika* **30** (11) 1019 – 1024 (2000)
Translated by E N Ragozin

## 2. Experiment

The electron impact excitation of the levels of the iron atom and singly charged ion was studied in the reactions

$$\mathrm{Fe} + \mathrm{e} \rightarrow \mathrm{Fe}^{*} + \mathrm{e}', \tag{2}$$

$$\mathrm{Fe} + \mathrm{e} \rightarrow \mathrm{Fe}^{+*} + \mathrm{e}' + \mathrm{e}'', \tag{3}$$

where e and e′ are the incident and scattered electrons and e″ is the electron knocked out of an iron atom upon its ionisation. The experiment was performed by the method of extended intersecting beams [9] by detecting the optical emission of atoms and ions excited in the beam intersection region.

To produce the atomic beam, the powder of carbonyl iron (extra pure grade TU-6-09-3000-73, class 6-2) with a total impurity content below 0.001 % was vaporised by electron beam heating. To remove physically adsorbed gases from the ramified surface of the powder particles and, what is equally important, to obtain a stable metal melt surface, the powder was subjected to prior melting and cast into a metal ingot. The ingot was placed into a graphite crucible, above a layer of the powder approximately 8 mm in thickness. The powder layer served as an efficient thermal insulator, thereby significantly reducing the power transferred from the melted metal to the crucible and, in addition, eliminating the diffusion of graphite in liquid iron and the formation of carbides.

For a surface temperature of the liquid metal of 1800 K, the atom density in the region of intersection of the beams amounted to $2.5 \times 10^{10}$ cm$^{-3}$. To detect intense resonance lines of Fe I located in the UV region near 250 nm, the atom density was lowered to $2 \times 10^{9}$ cm$^{-3}$ to minimise the reabsorption. For the Fe II lines, including the resonance lines, this precaution was insignificant because the ion content in the beam did not exceed $10^{-4}$ of the total number of atoms.

The iron atoms being vaporised occupy not only the ground $a\,^5D_4$ level, but also other levels of the ground $a\,^5D_{3,2,1,0}$ term. The population of these levels is determined both by the thermal excitation mechanism and the very process of atom escape from the melted metal. Strictly speaking, it is not thermodynamically equilibrium; nevertheless, when estimating the population densities of the low-lying levels of atomic iron, it is reasonable use the Boltzmann distribution, because a more rigorous calculation is extremely complicated. The estimates give the following population densities (in percent of the total atom density in the beam; the numbers in parentheses indicate the energy levels in inverse centimetres): 45.8 for $a\,^5D_4$ (0), 30.3 for $a\,^5D_3$ (415), 14.3 for $a\,^5D_2$ (704), 7.4 for $a\,^5D_1$ (888), and 2.2 for $a\,^5D_0$ (978). The population of the nearest excited level of the metastable $a\,^5F$ term with the energy $E = 6928$ cm$^{-1}$ is negligible.

The beam intersection region is approximately a rectangular parallelepiped measuring $13 \times 28 \times 200$ mm. Recorded are the photons emitted in the direction of the largest dimension of the intersection region. The width of the electron energy distribution at the entry into the electron collector is 0.9 eV for an energy of 100 eV and 1.0 eV for 20 and 200 eV (for 90 % of the electrons). The beam current density did not exceed 1.0 mA cm$^{-2}$ throughout the 0 – 200 eV working energy range. The real spectral resolution of the setup was $\sim 0.1$ nm in the short-wavelength part of the spectrum for $\lambda \leqslant 600$ nm; in the yellow-red spectral region, it was higher by about a factor of two because another diffraction grating was used in the monochromator. The spectral lines of atomic helium were used as the reference lines to determine the absolute cross section scale. To carry out the calibration, helium was admitted into the vacuum chamber instead of the atomic iron beam with the greatest possible retention of other experimental conditions that were not specific to the excitation of iron atoms or ions. These conditions, as well as check experiments, are described in detail in several previous papers [10 – 12].

The experimental error in determining the relative cross sections for the excitation of the spectral lines was from 3 to 12 %, depending on the line intensity and its position in the spectrum. The uncertainty in the determination of the absolute cross sections was between ±15 and ±24 %. The contributions of different error sources are discussed in greater detail in Ref. [10].

## 3. Results and discussion

About 800 cross sections for excitation of the spectral lines of atomic Fe in the 200 – 837 nm spectral range were measured for an energy of the exciting electrons of 50 eV. For the majority of lines, the OEFs were recorded in the 0 – 200 eV electron energy range. This paper presents the results pertaining to the three laser levels of Fe I indicated in the Introduction.

The diagram of the states of atomic iron is given in Fig. 1. The singlets, triplets, and septets are not presented in the diagram since all the laser transitions under discussion occur within the quintet energy diagram. To simplify the picture, the $J$ splitting of the terms is not shown, because it is relatively small for iron atoms. All the states located below 45000 cm$^{-1}$ are depicted, with the exception of the $v\,^5D^{\mathrm{o}}$ state which is partly overlapped with the $w\,^5D^{\mathrm{o}}$ state. The laser transitions mentioned in the Introduction are indicated by arrows. As regards even quintet states, apart from the $a\,^5P$, $a\,^5D$, and $a\,^5F$ states depicted in Fig. 1, the lowest of them, $e\,^5D$, has an energy of about 45000 cm$^{-1}$.

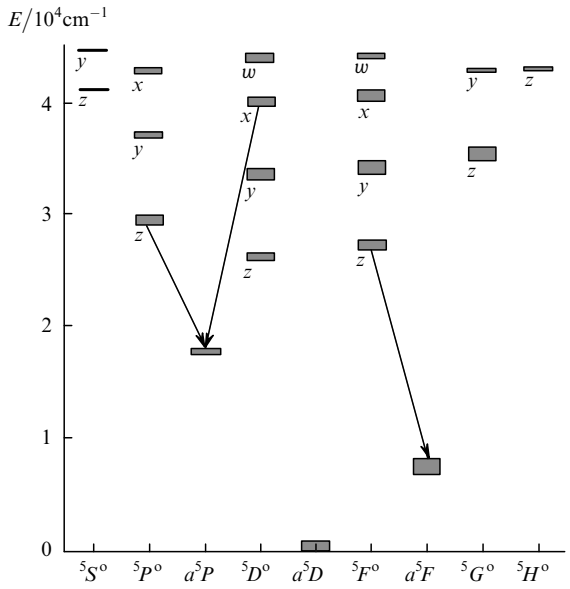


**Figure 1.** Diagram of the quintet states of atomic iron.

Although the cross section measurements by recording the optical emission of excited atoms yield directly the spectral-line excitation cross sections $Q_{ki}$, in the theory and many applied problems, the energy-level excitation cross sections $q_k$ are often used. These quantities are related by the expression

$$q_k = \sum_m Q_{km} - \sum_l Q_{lk}, \tag{4}$$

where the first sum takes into account the competition of the radiative transitions from the level $k$ (branching) and the second sum describes the cascade population of the level $k$ upon transitions from higher-lying levels. Because $Q_{ki}/Q_{km} = A_{ki}/A_{km}$, the data on transition probabilities can also be employed to take into account the branching. For many objects (atoms, ions), they are known more fully and with a higher precision than the information on the cross sections.

The cascade population is not considered in this work because the available data on the cascade transitions are not systematic in character. However, the author's experience gained with several other atoms and ions, for which the contribution of cascade transitions could be taken into relatively complete account suggests that the contribution of cascade transitions is typically 10 – 30 % of the total level excitation cross section.

The excitation cross sections for the three levels of atomic iron regarded in Refs [1 – 4] as upper laser levels are presented in Table 1. The excitation process investigated corresponds to reaction (2). Table 1 comprises all the known transitions from the levels under discussion. Shown therein are the upper (laser) and lower levels; the transition wavelength $\lambda$; transition probabilities $A_{ki}$ borrowed from Refs [5, 13]; excitation cross sections $Q_{50}$ for an electron energy of 50 eV; the ratio between the total probability $A^{\Sigma}_{\rm rec}$ of the transitions measured in this work, and the total probability $A^{\Sigma}_{\rm tot}$ of all the transitions known from Refs [5, 13], the total excitation cross section $Q^{\Sigma}_{50}$ for an electron energy of 50 eV; the total excitation cross section $Q^{\Sigma}_{\rm max}$ at the peak of the OEF; and the position $E(Q_{\rm max})$ of the peak. The last column contains references to the OEFs given in Fig. 2.

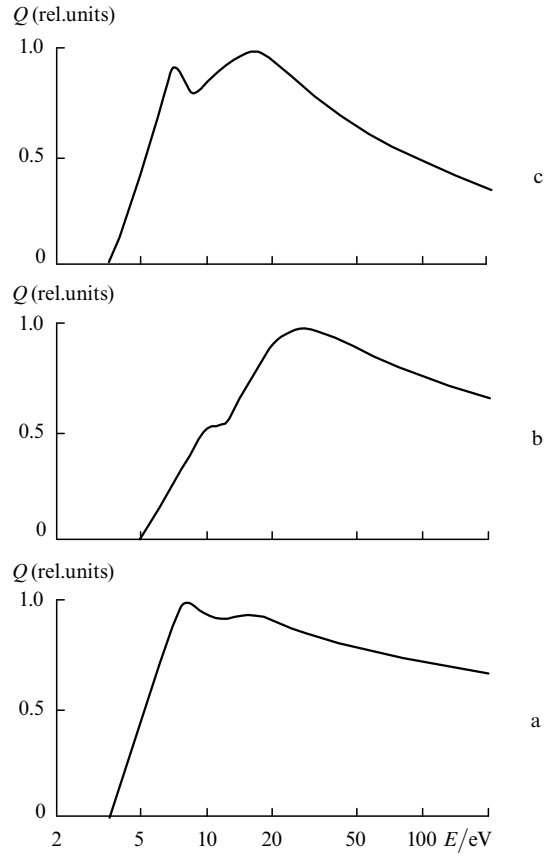


**Figure 2.** Normalised optical excitation functions Q for Fe I.

The ratio $A^{\Sigma}_{\rm rec}/A^{\Sigma}_{\rm tot}$ permits introducing corrections to the total cross sections to take into account the contribution of weak lines. However, one can see that the correction is significantly different from unity only for the $z\,^5P^{\rm o}_3$ level. At the same time, the absolute transition probabilities presented in Refs [5] and [13] are substantially different; in particular, for the laser transition in Fe I at 452.862 nm [4], the proba-

Table 1. Excitation cross sections of iron atoms.

| Upper level | Lower level | $\lambda$/nm | $A_{ki}/{\rm s}^{-1}$ [13] | $A_{ki}/{\rm s}^{-1}$ [5] | $Q_{50}/10^{-18}{\rm cm}^2$ | $A^{\Sigma}_{\rm rec}/A^{\Sigma}_{\rm tot}$ (%) | $Q^{\Sigma}_{50}/10^{-18}{\rm cm}^2$ | $Q^{\Sigma}_{\rm max}10^{-18}/{\rm cm}^2)$ | $E(Q_{\rm max})/{\rm eV}$ | OEF in Fig. 2 |
|---|---|---|---|---|---|---|---|---|---|---|
| $z\,^5P^{\rm o}_3$ | $a\,^5D_4$ | 344.061 | $1.71\times10^7$ | $4\times10^7$ | 10.8 | 94.4 | 18.7 | 23.6 | 7.5 | a |
| | $a\,^5D_3$ | 349.057 | – | $8.3\times10^6$ | 5.20 | | | | | |
| | $a\,^5D_2$ | 352.604 | – | $1.9\times10^6$ | 1.55 | | | | | |
| | $a\,^3F_4$ | 585.318 | $1.7\times10^2$ | – | – | | | | | |
| | $a\,^5P_3$ | 868.863 | – | $1.9\times10^6$ | – | | | | | |
| | $a\,^5P_2$ | 882.423 | – | $10^6$ | – | | | | | |
| $x\,^5D^{\rm o}_4$ | $a\,^5D_4$ | 252.285 | $2.9\times10^8$ | $3.2\times10^8$ | 36.5 | 99.6 | 56.9 | 63.4 | 28 | b |
| | $a\,^5D_3$ | 254.961 | $3.6\times10^7$ | $7.4\times10^7$ | 6.70 | | | | | |
| | $a\,^5F_5$ | 305.745 | $4.5\times10^7$ | $9\times10^7$ | 10.1 | | | | | |
| | $a\,^5F_4$ | 309.997 | – | – | 2.00 | | | | | |
| | $a\,^5F_3$ | 313.411 | $1.4\times10^7$ | – | – | | | | | |
| | $a\,^3F_4$ | 361.566 | $7.5\times10^4$ | – | – | | | | | |
| | $a\,^5P_3$ | 452.862 | $6.3\times10^6$ | $2\times10^7$ | 1.34 | | | | | |
| $z\,^5F^{\rm o}_5$ | $a\,^5D_4$ | 371.993 | $1.63\cdot10^7$ | $2.3\times10^7$ | 25.6 | 100 | 25.8 | 38.7, 41.6 | 6.7, 16 | c |
| | $a\,^5F_5$ | 501.207 | $5.5\times10^4$ | $6.1\times10^4$ | 0.20 | | | | | |
| | $a\,^5F_4$ | 512.736 | $1.14\times10^4$ | – | 0.05 | | | | | |

bilities $A_{ki}$ differ by a factor of 3.2. In the UV region at 250 nm, this difference becomes 2 – 1.1 times smaller. Nevertheless, we are forced to use the data of Ref. [5] because the authors of [5] give five values of $A_{ki}$ for transitions from the $z\,^5P_3^o$ level, whereas only two values of $A_{ki}$ are given in [13]. In addition, the error for the branching ratios of Ref. [5] is not as high as for the absolute probabilities $A_{ki}$.

Along with the atomic cross sections, 60 excitation cross sections for the spectral lines of a singly charged iron ion were also measured in this paper. The asymmetric charge exchange in reaction (1) involves the simultaneous ionisation of the iron atom and excitation of the singly charged ion. On the other hand, the selection of levels in Ref. [6] stems from a consideration of the processes corresponding to reaction (1). However, when some of the heavy rare gases (Ar and especially Kr) is used as a buffer gas, the process (1) will involve the efficient population of the Fe II levels with the energy of about 38000 – 48000 $cm^{-1}$. Upon excitation by the electron impact, the population of these levels is also much more likely to occur than the population of the levels considered in Ref. [6].

According to the data of Ref. [14], all odd levels of Fe II located in the above energy range belong to the $3d^6(^5D)4p$ configuration. The information on the electron-impact excitation cross sections for these levels obtained in this work is presented in Table 2. Here, the lower ($E_1$) and upper ($E_2$) energy levels are measured from the ground level of singly charged iron ion. Table 2 comprises only the terms that gave rise to the transitions for which the OEFs shown in Fig. 3 were recorded. The diagram of the states of Fe II (Fig. 4) shows the terms studied and the transitions arising from them (except the intersystem crossing to the doublet level $a\,^2P_{3/2}$, all the remaining transitions correspond to multiplets rather than to the individual lines).

One can see from these data that the measured excitation cross sections do not exceed $10^{-17}$ $cm^{-2}$. The excitation cross sections for quartet and sextet levels weakly differ in the magnitude. The OEF peaks are located far away from the excitation threshold. This circumstance could significantly increase the electron temperature required upon excitation of Fe II in a gas discharge. However, this should not present significant problems upon excitation by an electron beam with the energy of the order of several kiloelectronvolts.

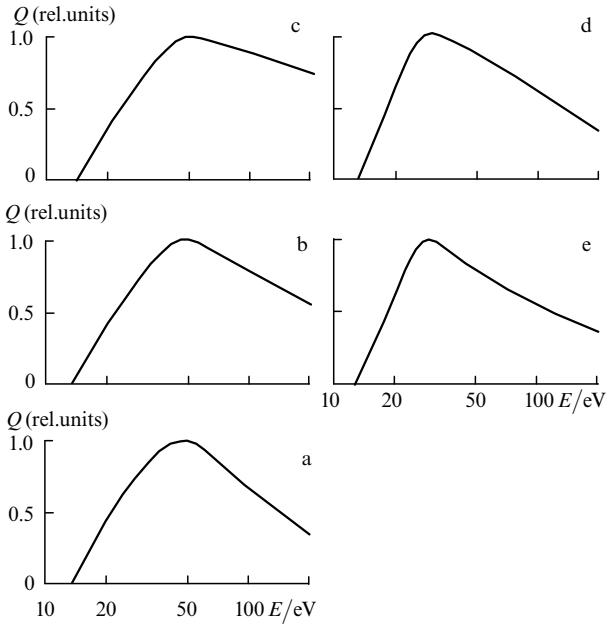


**Figure 3.** Normalised optical excitation functions Q for Fe II.

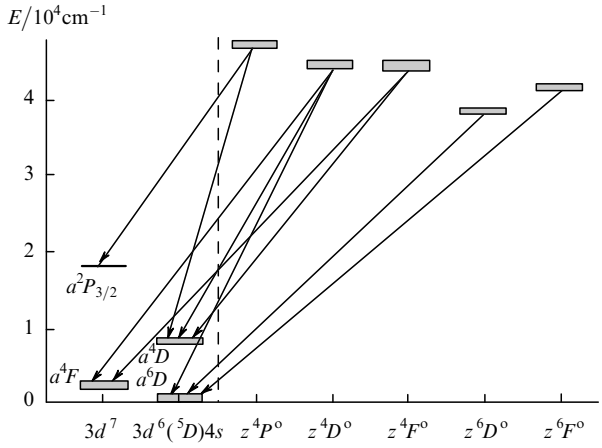


**Figure 4.** Energy level diagram of Fe II showing the transitions studied.

In the process (3), the initial atoms are in the $3d^64s^2\,a\,^5D$ state. Upon excitation to the odd levels of the $3d^6(^5D)4p$ configuration under study, one of the 4*s* equivalent electrons is removed, while another one undergoes the allowed $4s \rightarrow 4p$ transition. At the same time, the majority of low-lying even levels of Fe II (potentially, the lower laser levels) belong to the $3d^7$ configuration. The removal of one 4*s* electron with the simultaneous $4s \rightarrow 3d$ conversion of another electron is far less likely, which favours obtaining population inversion. However, two other low-lying terms of Fe II, $a\,^6D$ (the ground one) and $a\,^4D$, belong to the $3d^6(^5D)4s$ configuration and are likely to be efficiently populated by the electron impact in the process (3).

Note in conclusion that the lifetimes of 186 levels of Fe I, including two upper laser levels $z\,^5F_5^o$ and $x\,^5D_4^o$, were measured recently [15]. The transition probabilities for 478 spectral lines of Fe I were measured with a higher precision than in earlier papers. Unfortunately, none of the atomic iron laser lines, observed or assumed to lase, was among them. More recently [16], the $x\,^5D_4^o$ level lifetime $\tau$ measured in Ref. [15] was confirmed with a high accuracy. In addition, extended and improved data on the lifetimes of the $z\,^4P^o$, $z\,^4D^o$, $z\,^4F^o$, $z\,^6D^o$ [17] and $z\,^6P^o$, $z\,^6D^o$, $z\,^6F^o$ [18] levels were obtained for Fe II. All of these investigations were carried out employing laser-induced fluorescence. Accumulation of the information on atomic constants for Fe I and Fe II sets the stage for constructing a realistic physicomathematical model of an electron-beam-pumped laser on the transitions of Fe I and Fe II.

## References

1. Walter W T, Solimene N, Piltch M, Gould K *IEEE J. Quantum Electron.* **2** 474 (1966)
2. Petrash G G *Usp. Fiz. Nauk* **105** 654 (1971)
3. Linevsky M J, Karras T W *Appl. Phys. Lett.* **33** 720 (1978)
4. Divin V D, Isakov V K *Kvantovaya Elektron.* **11** 1038 (1984) [*Sov. J. Quantum Electron.* **14** (5) 700 (1984)]
5. Corliss C H, Bozeman W R *Experimental Transition Probabilities for Spectral Lines of Seventy Elements* (Washington, DC: US Government Printing Office, 1962)

Table 2. Excitation cross sections of singly charged iron ions.

| $\lambda$/nm | Transition | $J \rightarrow J'$ | $E_1$/cm$^{-1}$ | $E_2$/cm$^{-1}$ | $Q_{50}/10^{-18}$cm$^2$ | $Q_{max}/10^{-18}$cm$^2$ | $E(Q_{max})$/eV | OEF in Fig. 3 |
|---|---|---|---|---|---|---|---|---|
| 224.917 | $a^6D - z^4D^o$ | 9/2–7/2 | 0 | 44446 | 0.51 | 0.52 | 48 | b |
| 233.131 | $a^4F - z^4F^o$ | 9/2–7/2 | 1872 | 44753 | 0.41 | 0.41 | 50 | c |
| 234.810 | $a^4F - z^4D^o$ | 9/2–7/2 | 1872 | 44446 | 1.31 | 1.33 | 48 | b |
| 235.489 | $a^4F - z^4F^o$ | 5/2–3/2 | 2837 | 45289 | 0.20 | 0.20 | 50 | c |
| 236.000 | $a^4F - z^4F^o$ | 9/2–9/2 | 1872 | 44232 | 1.82 | 1.83 | 50 | c |
| 236.029 | $a^4F - z^4D^o$ | 7/2–5/2 | 2430 | 44784 | | | 48 | b |
| 236.202 | $a^4F - z^4F^o$ | 7/2–7/2 | 2430 | 44753 | 1.23 | 1.23 | 50 | c |
| 237.050 | $a^4F - z^4F^o$ | 3/2–3/2 | 3117 | 45289 | 0.55 | 0.55 | 50 | c |
| 237.373 | $a^6D - z^6F^o$ | 9/2–9/2 | 0 | 42114 | 0.61 | 0.72 | 28 | e |
| 237.928 | $a^4F - z^4D^o$ | 7/2–7/2 | 2430 | 44446 | 0.59 | 0.60 | 48 | b |
| 238.204 | $a^6D - z^6F^o$ | 9/2–11/2 | 0 | 41968 | 3.97 | 4.36 | 28 | e |
| 238.324 | $a^4F - z^4D^o$ | 5/2–5/2 | 2837 | 44784 | 0.34 | 0.34 | 48 | b |
| 238.438 | $a^4F - z^4D^o$ | 3/2–3/2 | 3117 | 45044 | 0.19 | 0.19 | 48 | b |
| 238.863 | $a^6D - z^6F^o$ | 7/2–7/2 | 384 | 42237 | 0.62 | 0.73 | 28 | e |
| 239.541 | $a^6D - z^6F^o$ | 5/2–3/2 | 667 | 42401 | 2.26 | 2.66 | 28 | e |
| 239.563 | $a^6D - z^6F^o$ | 7/2–9/2 | 384 | 42114 | | | 28 | e |
| 239.924 | $a^4F - z^4D^o$ | 3/2–5/2 | 3117 | 44784 | 0.55 | 0.60 | 48 | b |
| 239.924 | $a^6D - z^6F^o$ | 5/2–5/2 | 667 | 42334 | | | 28 | e |
| 240.443 | $a^6D - z^6F^o$ | 3/2–1/2 | 862 | 42439 | 0.95 | 1.12 | 28 | e |
| 240.448 | $a^6D - z^6F^o$ | 5/2–7/2 | 667 | 42237 | | | 28 | e |
| 240.666 | $a^6D - z^6F^o$ | 3/2–3/2 | 862 | 42401 | 0.39 | 0.46 | 28 | e |
| 241.052 | $a^6D - z^6F^o$ | 3/2–5/2 | 862 | 42334 | 0.77 | 0.91 | 28 | e |
| 241.107 | $a^6D - z^6F^o$ | 1/2–1/2 | 977 | 42439 | 0.25 | 0.29 | 28 | e |
| 241.331 | $a^6D - z^6F^o$ | 1/2–3/2 | 977 | 42401 | 0.53 | 0.62 | 28 | e |
| 256.253 | $a^4D - z^4P^o$ | 7/2–5/2 | 7955 | 46967 | 1.26 | 1.28 | 45 | a |
| 256.347 | $a^4D - z^4P^o$ | 5/2–3/2 | 8391 | 47389 | 0.86 | 0.88 | 45 | a |
| 256.691 | $a^4D - z^4P^o$ | 3/2–1/2 | 8680 | 47626 | 0.52 | 0.53 | 45 | a |
| 257.792 | $a^4D - z^4P^o$ | 1/2–1/2 | 8846 | 7626 | 0.30 | 0.31 | 45 | a |
| 258.259 | $a^4D - z^4P^o$ | 3/2–3/2 | 8680 | 47389 | 0.52 | 0.53 | 45 | a |
| 258.588 | $a^6D - z^6D^o$ | 9/2–7/2 | 0 | 38660 | 1.65 | 2.14 | 28 | d |
| 259.154 | $a^4D - z^4P^o$ | 5/2–5/2 | 8391 | 46967 | 0.71 | 0.73 | 45 | a |
| 259.373 | $a^4D - z^4P^o$ | 1/2–3/2 | 8846 | 47389 | 0.20 | 0.20 | 45 | a |
| 259.837 | $a^6D - z^6D^o$ | 7/2–5/2 | 384 | 38858 | 1.38 | 1.79 | 28 | d |
| 259.940 | $a^6D - z^6D^o$ | 9/2–9/2 | 0 | 38458 | 5.92 | 7.70 | 28 | d |
| 260.709 | $a^6D - z^6D^o$ | 5/2–3/2 | 667 | 39013 | 1.08 | 1.40 | 28 | d |
| 261.107 | $a^4D - z^4P^o$ | 3/2–5/2 | 8680 | 46967 | 0.39 | 0.40 | 45 | a |
| 261.187 | $a^6D - z^6D^o$ | 7/2–7/2 | 384 | 38660 | 4.30 | 5.59 | 28 | d |
| 261.382 | $a^6D - z^6D^o$ | 3/2–1/2 | 862 | 39109 | 0.68 | 0.88 | 28 | d |
| 261.762 | $a^6D - z^6D^o$ | 5/2–5/2 | 667 | 38858 | 2.85 | 3.83 | 28 | d |
| 262.167 | $a^6D - z^6D^o$ | 1/2–1/2 | 977 | 39109 | 0.92 | 1.20 | 28 | d |
| 262.567 | $a^6D - z^6D^o$ | 7/2–9/2 | 384 | 38458 | 1.76 | 2.29 | 28 | d |
| 263.105 | $a^6D - z^6D^o$ | 3/2–5/2 | 862 | 38858 | 1.97 | 2.56 | 28 | d |
| 263.132 | $a^6D - z^6D^o$ | 5/2–7/2 | 667 | 38660 | | | 28 | d |
| 273.697 | $a^4D - z^4D^o$ | 3/2–1/2 | 8680 | 45206 | 0.45 | 0.45 | 48 | b |
| 273.955 | $a^4D - z^4D^o$ | 7/2–7/2 | 7955 | 44446 | 5.87 | 5.93 | 48 | b |
| 274.648 | $a^4D - z^4F^o$ | 3/2–5/2 | 8680 | 45079 | 5.43 | 5.43 | 50 | c |
| 275.574 | $a^4D - z^4F^o$ | 7/2–9/2 | 7955 | 44232 | 9.22 | 9.22 | 50 | c |
| 349.467 | $a^2P - z^4P^o$ | 3/2–5/2 | 18360 | 46967 | 0.26 | 0.27 | 45 | a |

6. Johansson S, Litzen U *J. Phys. B: At. Mol. Opt. Phys.* **13** L253 (1980)
7. Johansson S *Phys. Scr.* **18** 217 (1978)
8. Arlantsev S V, Borovich B L, Buchanov V V, Yurchenko N I *Kvantovaya Elektron.* **23** 977 (1996) [*Quantum Electron.* **26** (11) 952 (1996)]
9. Smirnov Yu M *Fizika Elektronnykh i Atomnykh Stolknovenii* (The Physics of Electron and Atomic Collisions) (Leningrad: Physico-technical Institute, Acad.Nauk SSSR, 1985)
10. Smirnov Yu M *J. Phys. II* **4** 23 (1995)
11. Kuchenev A N, Smirnov Yu M *Phys. Scr.* **51** 578 (1995)
12. Kuchenev A N, Samsonova E A, Smirnov Yu M *Avtometriya* (5) 109 (1990)
13. Fuhr J R, Martin G A, Wiese W L, Younger S M *J. Phys. Chem. Ref. Data* **10** 305 (1981)
14. Reader J, Sugar J *J. Phys. Chem. Ref. Data* **4** 353 (1975)
15. O'Brian T R, Wickliffe M E, Lawler J E, Whaling W, Brault J W *J. Opt. Soc. Am. B: Opt. Phys.* **8** 1185 (1991)
16. Langhans G, Schade W, Helbig V *Z. Phys. D* **34** 151 (1995)
17. Hannaford P, Lowe R M *J. Phys. B* **16** L43 (1983)
18. Schade W, Mundt B, Helbig V *J. Phys. B* **21** 2691 (1988)